THE JOURNAL OF BIOLOGICAL CHEMISTRY VOL. 290, NO. 38, pp. 23110–23123, September 18, 2015

Characterization of P4 ATPase Phospholipid Translocases (Flippases) in Human and Rat Pancreatic Beta Cells

*THEIR GENE SILENCING INHIBITS INSULIN SECRETION**

Received for publication, March 26, 2015, and in revised form, July 30, 2015 Published, JBC Papers in Press, August 3, 2015, DOI 10.1074/jbc.M115.655027

Israr-ul H. Ansari[‡], Melissa J. Longacre[‡], Coen C. Paulusma[§], Scott W. Stoker[‡], Mindy A. Kendrick[‡], and Michael J. MacDonald[‡1]

From the [‡]Childrens Diabetes Center, University of Wisconsin School of Medicine and Public Health, Madison, Wisconsin 53706 and the [§]Tytgat Institute for Liver and Intestinal Research, Academic Medical Center, 1105 BK Amsterdam, The Netherlands

Background: Flippases translocate phosphatidylserine (PS) across lipid bilayers in secretory granules (SG) and plasma membranes (PM).
Results: Flippases were characterized in pancreatic beta cells, including in SG. Flippase knockdown inhibited insulin secretion.
Conclusion: Flippases play key roles in insulin secretion by rapidly moving PS across lipid bilayers.
Significance: PS couples fusion of SG with the PM to promote insulin exocytosis.

The negative charge of phosphatidylserine in lipid bilayers of secretory vesicles and plasma membranes couples the domains of positively charged amino acids of secretory vesicle SNARE proteins with similar domains of plasma membrane SNARE proteins enhancing fusion of the two membranes to promote exocytosis of the vesicle contents of secretory cells. Our recent study of insulin secretory granules (ISG) (MacDonald, M. J., Ade, L., Ntambi, J. M., Ansari, I. H., and Stoker, S. W. (2015) Characterization of phospholipids in insulin secretory granules in pancreatic beta cells and their changes with glucose stimulation. *J. Biol. Chem.* 290, 11075–11092) suggested that phosphatidylserine and other phospholipids, such as phosphatidylethanolamine, in ISG could play important roles in docking and fusion of ISG to the plasma membrane in the pancreatic beta cell during insulin exocytosis. P4 ATPase flippases translocate primarily phosphatidylserine and, to a lesser extent, phosphatidylethanolamine across the lipid bilayers of intracellular vesicles and plasma membranes to the cytosolic leaflets of these membranes. CDC50A is a protein that forms a heterodimer with P4 ATPases to enhance their translocase catalytic activity. We found that the predominant P4 ATPases in pure pancreatic beta cells and human and rat pancreatic islets were ATP8B1, ATP8B2, and ATP9A. ATP8B1 and CDC50A were highly concentrated in ISG. ATP9A was concentrated in plasma membrane. Gene silencing of individual P4 ATPases and CDC50A inhibited glucose-stimulated insulin release in pure beta cells and in human pancreatic islets. This is the first characterization of P4 ATPases in beta cells. The results support roles for P4 ATPases in translocating phosphatidylserine to the cytosolic leaflets of ISG and the plasma membrane to facilitate the docking and fusion of ISG to the plasma membrane during insulin exocytosis.

Our recent study that characterized the phospholipid composition of insulin secretory granules (ISG)[2] of pancreatic beta cells suggested that ISG phosphatidylserine (PS) facilitates docking and fusion of the ISG with the plasma membrane during insulin exocytosis (1). We found that the concentration of PS in ISG is 5-fold that of the whole cell, and with glucose stimulation its concentration in ISG increases even more (1). PS is the most abundant negatively charged phospholipid in most cells, including in the beta cell (1), and the concentration of PS in the plasma membrane of most cells is known to be high. The movement of PS from the inner (luminal) to the outer (cytosolic) leaflet of the ISG and from the outer to the cytosolic leaflet of the plasma membrane should facilitate docking of the ISG with the plasma membrane. The negative charge of PS facilitates the zippering interaction between the domains of positively charged amino acids of secretory vesicle SNARE proteins with similar domains of positively charged amino acids in the plasma membrane SNARE proteins in secretory cells (2–7). In the pancreatic beta cell, this should facilitate the docking and fusion of the ISG bilayer with the plasma membrane bilayer promoting insulin exocytosis. In support of this concept, mutations that reduce the net positive charge in the juxtamembrane lipid-binding domain of the vesicle SNARE protein VAMP2 interfere with the normal catecholamine release from chromaffin cells (3, 4) and inhibit secretion of insulin granules from pancreatic beta cells (6).

Because PS and other phospholipids are distributed asymmetrically in lipid bilayers of the plasma membrane and cell organelles and their rapid movement across lipid bilayers is energetically unfavorable, this led us to identify and investigate

* This work was supported in part by National Institutes of Health Grant DK28348. This work was also supported by the Nowlin Family Trust of the InFaith Community Foundation. The authors declare that they have no conflicts of interest with the contents of this article.
[1] To whom correspondence and reprint requests should be addressed: E-mail: mjmacdon@wisc.edu.

[2] The abbreviations used are: ISG, insulin secretory granule(s); BCH, 2-aminobicyclo[2,2,1]heptane-2-carboxylic acid; PS, phosphatidylserine; RNA-seq, RNA sequencing; qPCR, quantitative PCR.

enzymes that can influence the distribution and movement of PS across lipid bilayers in the beta cell. There are at least three categories of enzymes that influence lipid movements across bilayers. Flippases are P4 ATPases that translocate the aminophospholipids PS and, to a lesser extent, phosphatidylethanolamine against a concentration gradient from the outer leaflet to the cytosolic leaflet of the plasma membrane or, in the case of intracellular vesicles from the luminal (inside) leaflet, to the cytosolic (outer) leaflet of the lipid bilayer (8). Studies in *Saccharomyces cerevisiae* showed that P4 ATPases are important in vesicle biogenesis and are required for vesicular trafficking along several intracellular vesicular transport routes (8). These integral membrane proteins transfer the polar head of the aminophospholipid through the hydrophobic center of the lipid bilayer against a concentration gradient (8–15). Floppases use ATP to translocate the phospholipids phosphatidylcholine and sphingolipids, as well as cholesterol, across biological membranes in the opposite direction of flippases. Scramblases are ATP-independent and less substrate-specific and facilitate the movement of lipids along concentration gradients (8–15). Of the three types of enzymes that transport phospholipids across lipid bilayers, flippases seem the most relevant to the translocation of PS across the leaflets of the ISG lipid bilayer. In addition to facilitating coupling of the ISG membrane to the plasma membrane by translocating PS during insulin exocytosis, flippases could also promote insulin exocytosis through other mechanisms of PS action in the plasma membrane. On the plasma membrane inner leaflet, PS helps organize lipid rafts and can serve to recruit members of the protein kinase C family as well as signaling molecules containing hydrophobic side chains, such as Ras, Rho, and Src. In both the ISG and the plasma membrane, PS can induce local membrane curvature and recruit specific effector complexes that facilitate vesicle formation and trafficking (2, 11, 16–22). Interestingly, the discovery of PS flippase activity in bovine adrenal chromaffin granules led to the first purification and cloning of a P4 ATPase (23–25). In the trans-Golgi network, flippases are involved in vesicle biogenesis (8).

CDC50A, also called TMEM30, was recently discovered to be a β-subunit of P4 ATPases, which, upon heterodimerization with P4 ATPases, forms a phospholipid translocation complex (26–30). CDC50A has been localized by immunohistochemistry to secretory granules in both endocrine and exocrine cells of the pancreas (29).

In the current study, we characterized the expression of P4 ATPases and CDC50A in pure beta cells (the rat insulinoma INS-1 832/13 beta cell line) and human and rat pancreatic islets by initially measuring RNA levels with transcriptome sequencing (RNA-seq) and qPCR. We then estimated the protein levels of the P4 ATPases that showed the highest mRNA expression. Next, we used stable transfection of shRNA to generate beta cell lines with knockdown of the more abundant P4 ATPases as well as CDC50A in INS-1 832/13 cells in order to study the effect on secretagogue-stimulated insulin secretion. We also used virus-mediated delivery of shRNA to infect human pancreatic islets with shRNAs to target the abundant P4 ATPases and CDC50A to study their roles in glucose-stimulated insulin secretion in human pancreatic islets. ATPases ATP8B1, ATP8B2, and ATP9A were abundant in INS-1 832/13 cells and in human pancreatic islets and were expressed at moderate levels in rat pancreatic islets. CDC50A protein was highly expressed in human pancreatic islets and INS-1 832/13 cells. We found that these proteins, especially CDC50A and ATP8B1, were highly concentrated in ISG. ATP9A was concentrated in the plasma membrane and possibly also in the trans-Golgi network. Knockdown of these proteins in INS-1 832/13 cells and in human pancreatic islets inhibited glucose-stimulated insulin release and/or 2-aminobicyclo[2,2,1]heptane-2-carboxylic acid (BCH) plus glutamine-stimulated insulin release. This suggests that these enzymes play important roles in translocating PS and phosphatidylethanolamine in the ISG and plasma membrane lipid bilayers to facilitate fusion of the ISG membrane with the plasma membrane during insulin exocytosis in pancreatic beta cells. A presence in the trans-Golgi network would suggest a role in ISG biogenesis.

Experimental Procedures

Materials—Antibodies to ATP9A (catalogue no. sc-85287) and CDC50A (catalogue no. sc-133449) were from Santa Cruz Biotechnology, Inc. (Dallas, TX). An antibody to ATP9A (catalogue no. CSB-PA002422GA01HU from Cusabio (Wuhan, China) was used more frequently than the other antibody to ATP9A. An antibody to ATP8B1 (catalogue no. ab130441) was from Abcam (Cambridge, MA). Additional antibodies to APT8B1 and CDC50A were from Coen C Paulusma. The antibody to TGN38 (catalogue no. NBP1-03495) was from Novus Biologicals (Littleton, CO). Human pancreatic islets used in this study were from Prodo Laboratories Inc. and the Sharp-Lacy Research Institute (Irvine, CA) (two shipments used for immunoblots and six shipments used for insulin release) in addition to one from the University of Pennsylvania (used for insulin release) and one from the University of Illinois (used for immunoblot) supplied through the Integrated Islet Distribution Program. They were ≥90% pure and ≥90% viable. Male and female Sprague-Dawley rats were from Harlan Laboratories (Madison, WI). The INS-1 832/13 cell line was a generous gift from Chris Newgard (31). PIM(S) (Prodo islet medium) tissue culture medium was from Prodo Laboratories (catalogue no. S001GMP). Other chemicals were from Sigma in the highest purity available.

Construction and Sequencing of RNA Libraries—Total RNA samples from INS-1 832/13 cells were tested for purity and integrity verification (NanoDrop Spectrophotometer and Agilent 2100 BioAnalyzer, respectively) in preparation for RNA-seq library preparation. Each library was generated using Illumina's "TruSeq RNA Sample Preparation v2 Guide" (Illumina Part no. 15026495, Rev. C) and Illumina's TruSeq RNA Sample Prep Kit v2 (Illumina Inc., San Diego, CA). mRNA was purified from 1 μg of total RNA using poly-T oligo-attached magnetic beads. Subsequently, each mRNA sample was fragmented into small pieces using divalent cations under elevated temperature, and double-stranded cDNAs were synthesized using SuperScript II (Invitrogen) and random primers for first strand cDNA synthesis followed by second strand synthesis using DNA polymerase I and RNase H for removal of mRNA. Double-stranded cDNA was purified using Agencourt AMPure XP

TABLE 1
Nucleotide sequences of real-time RT-PCR primers used in this study

Gene ID	Primer name	Sequence
Rat		
Atb8b1 NM_001106140.1	Atp8b1-1037-F	5′-TTGTCCTCATCCTGGTTTCC-3′
	Atp8b1-1142-R	5′-GGTGTGGCATTTTCTCCATC-3′
Atp8b2 NM_001024798.2	Atp8b2-1357-F	5′-TCTTGGGATATGGGCTCAAC-3′
	Atp8b2-1456-R	5′-GGCGCTTTGTAAAAGGACTG-3′
Atp9a XM_002726282.2	Atp9a-1588-F	5′-ACAGAAAGCGTGGGACTGAC-3′
	Atp9a-1688-R	5′-AAGACCTGCAGGATGGTGAG-3′
Atp9b NM_001106130.1	Atp9b-1581-F	5′-GCCACGTCCTGAATTCCTAC-3′
	Atp9b-1672-R	5′-CGTTGAGGACTGGCTTCTTC-3′
Atp11a NM_001107324.2	Atp11a-1062-F	5′-AGCCACCCTCAAAAACACTG-3′
	Atp11a-1159-R	5′-TCTTTTGGGACTTGGATTGG-3′
Atp11b XM_001067830.3	Atp11b-1690-F	5′-TCAAACTGATGGCATTGGTG-3′
	Atp11b-1780-R	5′-AGCCTTTTCATCTGGTGACG-3′
Cdc50 NM_001004248.1	Cdc50-378-F	5′-GGATAACACGGCCTTCAAAC-3′
	Cdc50-487-R	5′-CGATGGGAATGAAGATGAGG-3′
Glud1 NM_008133.4	Glud1-F	5′-AACTACCACTTGCTCATGTCTG-3′
	Glud1-R	5′-TTCTCAGATGCACCCGATATCC-3′
Human		
ATP8B1 NM_005603.4	ATP8B1-1037-For	5′-GCAAATCCAGTCAGGGAAAG-3′
	ATP8B1-1142-Rev	5′-GAGGCTGCCTGGTAGTTGAG-3′
ATP8B2 NM_020452.3	huATP8B2-1331-F	5′-GCCACAGCTATGGTGATGTG-3′
	huATP8B2-1426-R	5′-CAGCCAGAGGATTGAAGGAG-3′
ATP9A BC110591.1	huATP9A-1237-F	5′-GATTTTCAAACGGCTCCATC-3′
	huATP9A-1334-R	5′-GGGATTGCTGGGTGTAAATG-3′
ATP9B NM_198531.3	huATP9B-1367-F	5′-GACCAGCACTATCCCAGAGG-3′
	huATP9B-1467-R	5′-GGTGCAGCCGCTTAAATATC-3′
ATP11A NM_015205.2	huATP11A-372-F	5′-CAAGCGGACTTCCACTCTTC-3′
	huATP11A-471-R	5′-CACTGGTTCATGGCATTGTC-3′
ATP11B XM_005247241.1	huATP11B-720-F	5′-CTGCAGACTTGGTGCTTCTG-3′
	huATP11B-821-R	5′-CTGCCACATGTGTCTTCAGG-3′
CDC50 BC009006.1	huCDC50A-01-F	5′-ATGGCGATGAACTATAACGCGAAG-3′
	huCDC50A-98-R	5′-TATCCGGTCTCCGAGTCTTC-3′
GLUD1 NM_005271.3	GLUD1-For	5′-CAAATCCAACGCACCCAGAG-3′
	GLUD1-Rev	5′-CTGTCACTCCTCCAGCATTCAAG-3′

beads (Beckman Coulter). cDNAs were end-repaired by T4 DNA polymerase and Klenow DNA polymerase and phosphorylated using T4 polynucleotide kinase. The blunt-ended cDNA was purified using Agencourt AMPure XP beads. The cDNA products were incubated with Klenow DNA polymerase to add an "A" base (adenine) to the 3′-end of the blunt phosphorylated DNA fragments. DNA fragments were ligated to Illumina adapters, which have a single "T" base (thymine) overhang at their 3′-end. The adapter-ligated products were purified using Agencourt AMPure XP beads. Adapter-ligated DNA was amplified in a linker-mediated PCR for 11 cycles using Phusion™ DNA polymerase and Illumina's PE genomic DNA primer set and then purified using Agencourt AMPure XP beads.

The quality and quantity of the finished libraries were assessed using an Agilent DNA 1000 series chip assay and QuantIT PicoGreen dsDNA kit (Invitrogen), respectively, and libraries were standardized to 2 μM. Cluster generation was performed using standard Cluster Kits (version 3) and the Illumina Cluster Station. Paired end 100-bp sequencing was performed using standard SBS chemistry (version 3) on an Illumina HiSeq2000 sequencer at the University of Wisconsin Biotechnology Center (Madison, WI). Images were analyzed using the standard Illumina Pipeline, version 1.8.2. The average number of reads/sample was 50 million. Results were analyzed by the Bioinformatics staff of the University of Wisconsin Biotechnology Center.

RNA Isolation and Quantitative RT-PCR—Total RNA from INS-1 832/13 cells and human and rat pancreatic islets, was isolated with the RNeasy minikit (Qiagen) protocol with on-column DNase digestion (RNase-free DNase set, Qiagen). To perform the cDNA synthesis and subsequent qPCR, total RNA was reverse transcribed using the RETRO-script kit (Ambion, Life Technologies) and oligo(dT) primers. The cDNA was used for real-time qPCR using the Bio-Rad MyIQ instrument with SYBR Premix Ex Taq (Takara Bio). Gene-specific forward and reverse primers along with a Fluorescein reagent (catalog no. 170-8780, Bio-Rad) were used to estimate individual mRNA levels. The cDNA derived from the pHygC cell line was used to make a standard curve using the rat glutamate dehydrogenase 1 gene (*Glut1*) as an internal control for rat islet and INS-1 832/13 samples (32–34). Similarly, cDNA from human pancreatic islets was used to make a standard curve with the human glutamate dehydrogenase 1 gene (*GLUD1*) for human islet samples. The quantitative RT-PCR primers to measure the various rat and human P4 ATPase mRNAs are listed in Table 1 (experiment shown in Fig. 1.).

Homogenates of Cells and Protein Concentration—For dilution to the optimal concentrations of cell protein to use for immunoblot analysis, it was practical to homogenize INS-1 832/13 cells (or human islets at a concentration of ~7,000 islets/ml) in KMSH solution (220 mM mannitol, 70 mM sucrose, and 5 mM potassium Hepes buffer, pH 7.5) with or without 1 mM dithiothreitol (32, 33) to produce a homogenate with about 2 mg of whole-cell protein/ml that was diluted as needed at the time of use. Protease inhibitor mixture (Thermo Scientific, catalogue no. 78415) was included in the homogenization solution. Rat islets were isolated as described previously (32–36) and homogenized in the KMSH solution described above, except the concentration of islets was about ~3,600 islets/ml of

homogenizing solution. The protein concentrations of whole-cell homogenates and supernatant fractions used for measurements of enzyme activity and immunoblot analysis were measured by the Bradford method.

Subcellular Fractionation of INS-1 832/13 Cells—Plates (150 mm) of monolayers of INS-1 832/13 cells were placed on ice and quickly washed twice with cold phosphate-buffered saline. Cells were scraped from the plates into a 1.5-ml microcentrifuge test tube and centrifuged at 600 × *g* for 20 s. All subsequent steps were at 4 °C. To obtain ISG, subcellular fractions were prepared with slight modifications of our (35–39) and others' (40–43) previously described methods. The cell pellet was suspended in 1 ml of KMSH containing 0.5 mM EGTA, 0.5 mM EDTA, and protease inhibitor (per one or two 150-mm plates of cells) and homogenized with 40 strokes up and down in a Potter-Elvehjem homogenizer. The method was designed to obtain pure ISG free from mitochondria and resulted in slight contamination of mitochondria with ISG and no contamination of ISG with mitochondria (Fig. 2) (1). The homogenate was centrifuged at 600 × *g* for 10 min, and the resulting supernatant fraction was centrifuged at 12,000 × *g* for 10 min to generate a mitochondrial pellet. The supernatant fraction from this centrifugation was centrifuged at 20,800 × *g* for 20 min to generate the insulin granule pellet (experiments shown in Figs. 4 (*A*, *B*, and *D*) and 5*C*). This pellet was washed up to three times with the homogenization solution described above with centrifugation at 20,800 × *g* for 20 min. The resulting ISG were judged to be >90% pure (1).

Granules used in some experiments were further purified on a sucrose gradient or a Nycodenz gradient (Accurate Chemical). To purify the granules on a sucrose gradient, the ISG pellet was resuspended in 200 μl of homogenization solution and overlaid on top of a discontinuous gradient prepared by layering 300-μl volumes of 60, 50, 45, 40, 30, and 20% (w/v) sucrose in a Beckman centrifuge test tube (11 × 34 mm). The test tube was centrifuged at 75,000 × *g* in a TLS-55 swinging bucket rotor in a Beckman TL-100 centrifuge at 4 °C for 3 h. Following this centrifugation, 250-μl fractions were collected from the top of the gradient down. The collected fractions were diluted with 1.75 ml of KMSH solution and centrifuged again at 100,000 × *g* for 30 min in a TLA-100.2 fixed angle rotor. The resultant pellets were resuspended in 30 or 50 μl of KMSH solution and used for further analyses. Granules were also further purified on a Nycodenz gradient using modifications to a previously published protocol (44). A discontinuous gradient was prepared by layering 600-μl volumes of 23.8, 8.8, and 4.4% (w/v) Nycodenz in a Beckman centrifuge tube (11 × 34 mm) as described above. The 200-μl granule sample purified by differential centrifugation described above was overlaid on top of the gradient and centrifuged at 75,000 × *g* at 4 °C for 3 h. Fractions of 250 μl were collected from the top of the gradient. These fractions were diluted with 1.75 ml of KMSH solution and centrifuged again at 100,000 × *g* for 30 min. The resultant pellets were resuspended in KMSH solution and used for further analyses (experiments shown in Figs. 3 and 4*D*).

To further purify a low density membrane fraction containing plasma membrane and trans-Golgi network, the post-ISG (20,800 × *g* for 20 min) supernatant fraction described above was centrifuged at 35,000 × *g* for 10 min. The resulting supernatant fraction was centrifuged at 130,000 × *g* for 1 h. The pellet from this centrifugation was suspended in 200 μl of KMSH solution and overlaid on top of the discontinuous sucrose gradient described above and centrifuged at 75,000 × *g* for 1.5 h. After the run, fractions of 250 μl were collected from the top of the gradient down, diluted with 1.75 ml of KMSH solution, and centrifuged again at 100,000 × *g* for 30 min. The resulting pellets were resuspended in 50 μl of KMSH solution and used for further analyses shown in Fig. 5*D*.

In addition, an alternative method for separating the plasma membrane from the trans-Golgi network was attempted by overlaying a post-nuclei and cell debris subcellular fraction (obtained by centrifuging the INS-1 832/13 whole cell homogenate at 600 × *g* for 10 min) on the sucrose gradient described above and centrifuging at 100,000 × *g* for 3 h (used in the experiment shown in Fig. 5*E*).

Immunoblot Analysis—Because the substrate(s) for the various P4 ATPases is the same, measurements of enzyme activity cannot distinguish among the various ATPases. Therefore, immunoblotting was performed to characterize these proteins in pure beta cells and pancreatic islets. Immunoblotting was performed as described previously (32–34, 36). Proteins were separated by SDS-PAGE, and after transfer to nitrocellulose, the membrane was blocked with a mixture of 10 mM Tris buffer, pH 8.0, and 150 mM NaCl (TBS) containing 5% nonfat powdered dry milk (for ATP9A, CDC50, and mitochondrial glycerol phosphate dehydrogenase) or TBS containing 3% bovine serum albumin (for ATP8B1) and probed with the primary antibody overnight at 4 °C. The next day, the membrane was washed and incubated with horseradish peroxidase-conjugated goat anti-rabbit IgG (Thermo Scientific) at a dilution of 1:15,000 for 40 min. The membrane was then washed with TBS, and the signal was detected using the Immobilon Western chemiluminescent HRP developer (Millipore catalogue no. WBKLS0100) for ATP9A and mitochondrial glycerol phosphate dehydrogenase and CDC50 and the Immun-Star HRP Luminol/Enhancer (Bio-Rad catalogue no. 170-5040) for ATP8B1. As a control for equal protein loading when samples of whole cells were compared, the blot was stripped with Restore Western blot stripping buffer (Thermo Scientific) and reprobed with a polyclonal antiserum to β-actin (catalogue no. B7653, Sigma-Aldrich) diluted in TBS containing 3% bovine serum albumin at a concentration of 1:10,000 overnight at 4 °C. The next day, the membrane was washed with TBS and incubated with horseradish peroxidase-conjugated goat anti-rabbit IgG (Thermo Scientific), used at a dilution of 1:15,000 for 40 min. The membrane was then washed with TBS, and the signal was detected using the West Pico CL kit (Pierce, catalogue no. 34077). To estimate relative densities of the protein bands captured on x-ray films exposed to the immunoblots, the areas and densities of the bands were measured with a Bio-Rad Chemidoc XRS+ imaging system and calculated with Image Lab software.

Marker Enzyme Assays—Assays were performed in 96-well plates (Fisherbrand® flat bottom, clear, polystyrene) and read in a Molecular Devices SpectraMax M2 microtiter plate reader. Alkaline phosphodiesterase I was measured as described previously (45, 46) in a 50-μl final volume of an enzyme reaction

mixture containing 1 mM sodium thymidine 5′-monophosphate *p*-nitrophenyl ester (Sigma), 1 mM $MgCl_2$, and 20 mM Tris-Cl buffer, pH 9, and 10 μl of enzyme source (1–10 μg of protein). After 15 min at 37 °C, the reaction was stopped by adding 50 μl of 0.8 M NaOH, and the absorbance of the mixture was read at 400 nm. The activity without thymidine 5′-monophosphate *p*-nitrophenyl ester in the reaction mixture was subtracted from the activity with thymidine 5′-monophosphate *p*-nitrophenyl ester to give the rate attributable to the phosphodiesterase. NADPH cytochrome *c* reductase was measured as described previously (45, 47) in a continuous spectrophotometric assay in 200 μl of reaction mixture containing 1 mM EDTA, 36 μM cytochrome *c* (Sigma-Aldrich), and 50 mM potassium phosphate buffer, pH 7.6, and 10 μl of enzyme source (1–15 μg of protein) at 550 nm at room temperature. After a background rate was obtained for about 1 min, the enzyme reaction was started by the addition of 20 μl of 1 mM NADPH to give a final concentration of 0.1 mM NADPH. The background rate in the absence of NADPH was subtracted from the total rate in the presence of NADPH to give the rate attributable to the reductase.

Mass Spectrometry Analysis of ISG Proteins—Proteins were characterized at the Mass Spectrometry Facility (Biotechnology Center, University of Wisconsin, Madison, WI) according to a previously described procedure (48). Proteins were extracted from SDS-lysed insulin granules and digested with trypsin. The resulting peptides were analyzed by nano-LC-MS/MS using the Agilent 1100 nanoflow system (Agilent Technologies) connected to a hybrid linear ion trap-orbitrap mass spectrometer (LTQ-Orbitrap XL, Thermo Fisher Scientific) equipped with a nanoelectrospray ion source. Files were searched against an NCBInr Rodent database (224,530 protein coding genes) using an in-house Mascot search engine version 2.2.07 (Matrix Science). Peptide mass tolerance was set at 20 ppm, and fragment mass was set at 0.8 Da. Protein annotations, significance of identification, and spectral based quantification was done with Scaffold software (version 3.6.3, Proteome Software Inc., Portland, OR). Protein identifications were accepted if they could be established at greater than 95.0% probability within a 1% false discovery rate and contained at least two identified peptides. Protein probabilities were assigned by the Protein Prophet algorithm (49).

shRNA Expression Vectors and Constitutively Expressing Cell Lines—shRNA expression vectors were generated in the vector pSilencer 2.1U6 Hygro + Tol2 (32, 50). The rat shRNA sequences were derived from mRNA sequences of *Atp8b1* (accession number NM_001106140.1), *Atp8b2* (accession number NM_001024798.2), *Atp9a* (accession number XM_002726282.2), and *Cdc50a* (accession number NM_001004248.1). The nucleotide target sequences of the shRNAs are listed in Table 2. To generate constitutively expressing shRNA in pure beta cells of the rat insulinoma cell line INS-1 832/13, cells were transfected with plasmid DNA using Lipofectamine 2000 (Life Technologies, Inc.). All transfections included an equimolar amount of the pCMV-Tol2 vector, which encodes the Tol2 transposase, to increase efficiency of transfection (32, 50). The next day, the complete growth medium was replaced with medium containing 150 μg/ml hygromycin B (Invivogen) and further incubated. The selection medium was replaced every 4 days, and cells were selected for about 15 days. The selected cell colonies were trypsinized and harvested and analyzed for gene-specific mRNA levels using qPCR and protein levels by immunoblot assay. In a similar way, a control cell line was also generated using a scrambled shRNA sequence and used as a control in all assays and designated pHyg-C (ACTACCGTTGTTATAGGTG). All insert sequences were confirmed by DNA sequencing. The resulting plasmids were transfected into the cell line INS-1 832/13 using Fugene HD (Roche Applied Science) according to product directions (32). Selection was maintained until testing.

TABLE 2
Nucleotide sequences of shRNA oligonucleotides used in this study

Gene	Oligonucleotide	shRNA sequence
Rat		
Atp8b1	Atp8b1-127	GAACAGAATCGTGTCAACAGA
	Atp8b1-465	GGCAATCAAAGACCTGGTAGA
	Atp8b1-1332	GCTAGGGCAGATCCATTACAT
Atp8b2	Atp8b2-1057	GGGAAGACACCGTCTTCAATG
	Atp8b2-2323	GGGCGTACTTCAACATCTA
	Atp8b2-3438	GCTTGGTGAATAAGTATTACC
Atp9a	Atp9a-289	GTTCAGATACTTCTTCAACT
	Atp9a-499	GACCGTGAAGGTGAAGAGT
	Atp9a-901	GCGGAGTGTCATGAATACTT
Cdc50a	Cdc50a-589	GTGAAATCCCGAGATGATA
	Cdc50a-1016	GTCTTATAGAGCGGACAGA
	Cdc50a-1172	GAATTGCTTACATCACTATT
Human		
ATP8B1	ATP8B1-322	GCAAACGATCGCAAGTACCA
	ATP8B1-1735	GTGGATAGGACTGATGGTCA
ATP9A	ATP9A-189	GGTATCCTCGGAATGTCAT
	ATP9A-1487	GAGAAGCAGTACGAAGACT
CDC50A	CDC50A-201	GACTCGGAGACCGGATAACA
	CDC50A-694	GAACGATTTAAAGGTACAACA

Lentiviruses Expressing shRNAs Targeting Human P4 ATPases—shRNA targets were cloned into pLVX1-shRNA1, and their sequences were confirmed by nucleotide sequencing. The pseudopackaged lentiviruses were recovered using the Lenti-X shRNA expression system (catalogue no. 632177, Clontech), following the manufacturer's protocol. The vector DNA along with packaging mix was transfected into 293T cells. After 4 h, the transfection medium was replaced with complete medium, and the cells were further incubated for 48 h. The clarified supernatant was collected, and the viral titer was measured by plaque-forming assays. To measure the viral titer, the clarified supernatant was serially diluted and overlaid onto INS-1 832/13 cells in 6-well plates. After virus adsorption for 1 h at 37 °C, the medium was replaced with complete growth medium containing 0.5 μg/ml puromycin. The plates were further incubated at 37 °C with medium changes. After 10 days, the medium was aspirated, and resistant colonies were stained with 1 ml of staining solution (0.01% crystal violet, 19% methanol). After 1 h, the staining solution was removed, and cell colonies were washed with water, air-dried, and counted to assign viral titers. Small aliquots of viral stock solution were stored at −80 °C for future use. The human shRNA sequences were derived from mRNA sequences with the accession numbers for *ATP8B1* (NM_005603.4), *ATP8B2* (NM_020452.3), *ATP9A* (BC110591.1), *ATP9B* (NM_198531.3), *ATP11A* (NM_015205.2), *ATP11B* (XM_005247241.1), and *CDC50A* (BC009006.1). The shRNA nucleotide target sequences are listed in Table 2.

Insulin Release with Cell Lines—The INS1–832/13 cells containing either control shRNA or target shRNA were tested for insulin release as described previously (32). In brief, ~0.5×10^6 INS-1 832/13 cells/well were plated in 24-well plates in quadruplicate for each cell line and test condition. Cells were maintained in RPMI 1640 cell culture medium (contains 11.1 mM glucose), 1 mM pyruvate, and 50 μM β-mercaptoethanol and 10% fetal calf serum. Twenty hours before an experiment, the medium was adjusted to contain 5 mM glucose and no pyruvate or β-mercaptoethanol (31, 32). On the day of the experiment, the medium was replaced with Krebs-Ringer bicarbonate buffer containing 3.0 mM glucose and 0.5% BSA and incubated for 2 h. The cells were washed once with Krebs-Ringer HEPES buffer BSA solution and further incubated with 1 ml of the same solution for 1 h at 37 °C in the presence or absence of 11.2 mM glucose or BCH (10 mM) plus glutamine (10 mM). Samples of medium were collected from each well and briefly centrifuged to eliminate any floating cells in the supernatant fraction and used for measurements of insulin. Results are the means ± S.E. insulin release of 16 or more replicate incubations/condition (quadruplicate replications per cell preparation performed on 4 or more separate days). Insulin was measured by radioimmunoassay with rat insulin as a standard.

Insulin Release with Human Pancreatic Islets—After human islets were received, the islets were incubated in PIM(S) supplemented with 1× penicillin/streptomycin at 37 °C. After 2–3 h of incubation, the islets were divided into portions. Each portion was incubated with a different lentivirus at a multiplicity of infection of 3 in the presence of 4 μg/ml Polybrene in PIM(S) islet medium for 2–3 h at 37 °C. The islets received a lentivirus carrying scrambled shRNA or lentiviruses carrying shRNA directed against a human P4 ATPase or CDC50A. Islets were then incubated in PIM(S). After 3 days, islets were used for insulin release experiments and for measurements of mRNA by qPCR. Insulin release was studied as described previously (34) with seven islets of the same average size per vial incubated for 1 h in the presence of 16.7 mM glucose in Krebs Ringer bicarbonate buffer modified to contain 10 mM Hepes buffer, pH 7.3, and 0.5% fatty acid-free bovine serum albumin. Insulin was measured by a radioimmunoassay with human insulin as a standard.

Statistical Significance—Statistical significance of differences was confirmed by Student's unpaired *t* test.

Results

Flippase mRNA Expression in Beta Cells and Pancreatic Islets—RNA-seq was used to study cDNA libraries made from INS-1 832/13 cells in order to obtain preliminary clues about which flippase mRNAs might be expressed in pure beta cells. According to this analysis, mRNAs of P4 ATPases (relative expression with highest = 100% shown in parentheses) *Atp11b* (100%), *Atp9a* (93%), and *Atp8b1* (53%) were highly expressed. *Atp9b* (22%) and *Atp8b5* (23%) (not present in humans (6)) showed intermediate expression, and *Atp11c* (6%), *Atp11a* (2%), *Atp8a1* (3%), *Atp8a2* (1%), and *Atp10d* (2%) showed very low expression.

To obtain a more specific measurement of the relative levels of P4 ATPase expression, qPCR was used to determine P4 ATPase mRNA levels in INS-1 832/13 cells and human and rat pancreatic islets. This showed relatively high expression of mRNAs of *Atp8b1*, *Atp8b2*, and *Atp9a* in INS-1 832/13 cells and rat pancreatic islets and of *ATP9A* in human pancreatic islets. The expression of *ATP11B* was low in all three types of cells, and the expression of *ATP9B*, *ATP11A*, and *ATP8B5* was very low in all three cell types (Fig. 1). The levels of mRNAs of *ATP8B1*, *ATP8B2*, and *ATP9A* in human islets relative to the level of the internal control mRNA, which was glutamate dehydrogenase mRNA, were lower in human islets than in the other two types of cells (Fig. 1). Relatively lower expression of the three mRNAs might have been due to a higher relative expression of glutamate dehydrogenase mRNA in the human pancreatic islets compared with the other two types of cells. This is likely because the protein levels of the P4 ATPases were higher in human islets relative to INS-1 832/13 cells and rat pancreatic islets as judged by immunoblotting (see below).

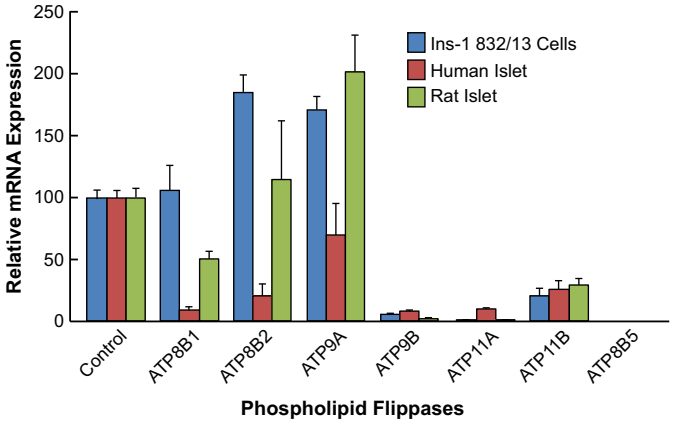

FIGURE 1. **mRNA levels of *ATP8B1*, *ATP8B2*, and *ATP9A* suggest that they are the predominant P4 ATPase flippases in INS-1 832/13 cells and rat and/or human pancreatic islets.** qPCR was used to estimate the mRNA levels relative to glutamate dehydrogenase mRNA as a control in the same tissue. Results are the mean ± S.E. (*error bars*) of three separate cell preparations of each cell type.

RNA-seq data showed *Cdc50a* mRNA is highly expressed in INS-1 832/13 cells (data not shown). qPCR also showed that the level of *CDC50A* mRNA is high in human islets (data not shown).

ATP8B1, ATP9A, and CDC50A were further characterized by estimating their protein levels in INS-1 832/13 cells, including in ISG, and human pancreatic islets. We also severely knocked down the mRNAs that encode these enzymes as well as *ATP8B2* mRNA with shRNA technology in INS-1 832/13 cells and human pancreatic islets.

Flippases ATP8B1, ATP8B2, ATP9A, and CDC50A Are Found in Pure Beta Cells and Pancreatic Islets and Are Concentrated in ISG and Plasma Membrane of Beta Cells—In addition to determining which P4 ATPases are present in beta cells, we attempted to discern the intracellular location(s) of the major P4 ATPases. Because previous work demonstrated that PS is concentrated in ISG (1) and PS is the major phospholipid translocated across cellular membranes by P4 ATPases, we developed a scheme for preparation of ISG designed to obtain pure granules, by sacrificing the yield of ISG in order to obtain more pure ISG completely free of mitochondria. Mitochondrial contamination of ISG has been a major problem with purification

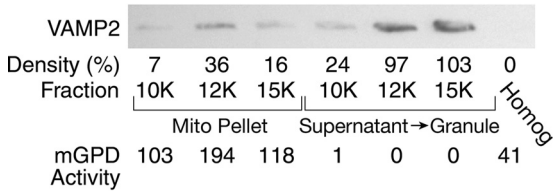

FIGURE 2. **No contamination of insulin secretory granule preparations with mitochondria.** The intention was to obtain pure insulin granules not contaminated with mitochondria as was the case with many previously used methods of obtaining insulin granules by differential centrifugation and gradient centrifugation. INS-1 832/13 cells were homogenized and fractionated as described under "Experimental Procedures." The post-nuclear/cell debris pellet from the 600 × *g* 10-min centrifugation was centrifuged at 10,000 × *g*, 12,000 × *g*, or 15,000 × *g* for 10 min to generate mitochondrial pellets. The resulting postmitochondrial supernatant fractions were then centrifuged at 20,000 × *g* for 20 min to generate insulin granule pellets. VAMP2 was analyzed by immunoblot analysis as a marker for insulin secretory granules. Mitochondrial glycerol phosphate dehydrogenase (*mGPD*) (one of the most highly expressed enzymes in pancreatic beta cells (51)) enzyme activity (nmol of product/mg of protein) is shown as a marker for mitochondria. VAMP2 and mitochondrial glycerol phosphate dehydrogenase levels in the whole cell homogenate (*Homog*) are shown also. The figure shows that the 12,000 × *g* supernatant fraction used to obtain purified insulin secretory granules has the insulin secretory granule marker VAMP2 present at a high concentration and no mitochondrial glycerol phosphate dehydrogenase. The presence of some VAMP2 in the mitochondrial pellet shows that this method of insulin granule purification results in some contamination of the mitochondrial pellet with insulin granules, as was expected.

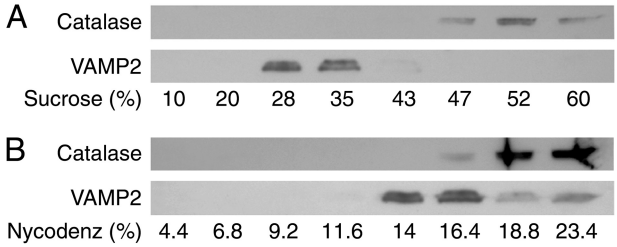

FIGURE 3. **Purification of ISG by sucrose and Nycodenz gradient centrifugation.** The ISG subcellular fraction obtained by differential centrifugation was further purified by sucrose (*A*) or Nycodenz (*B*) gradient centrifugation. The figure shows immunoblots simultaneously probed on the same immunoblot membrane for VAMP2, a marker for ISG, and for catalase, a marker for peroxisomes. The space on the blots between the higher molecular weight catalase and the lower molecular weight VAMP2 was completely blank and was removed from the picture. Percentages of sucrose in the cuts or Nycodenz in cuts 1–8 of the gradients are shown.

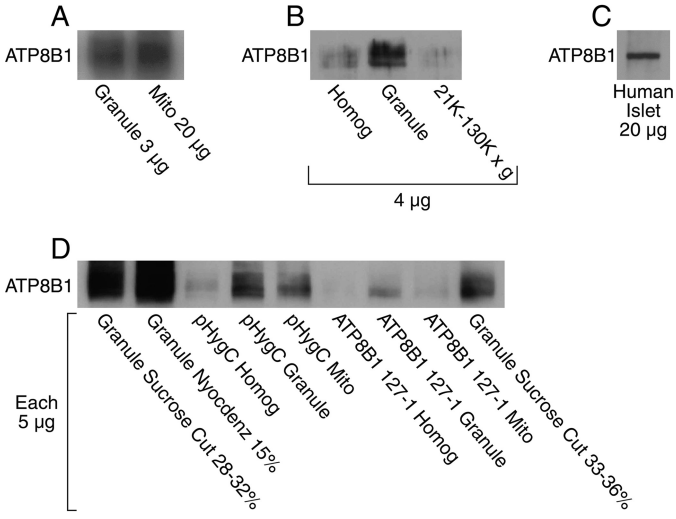

FIGURE 4. **ATP8B1 protein is present in INS-1 832/13 cells and human pancreatic islets and is concentrated in ISG of pure beta cells; gene silencing lowers ATP8B1 protein in ISG.** *A*, immunoblot with 3 or 20 μg of protein/lane. ATP8B1 appears as a broad band due to multiple glycosylated forms. Because some of the ISG contaminate the mitochondria according to the design of our subcellular fractionation procedure (see "Experimental Procedures"), some or most of the ATP8B1 in the mitochondrial (*Mito*) preparation could be from ISG. *B*, ATP8B1 is concentrated in ISG and not in plasma membrane, microsomes, or trans-Golgi network. The figure shows that ATP8B1 is present in a homogenate of whole INS-1 832/13 cells (*Homog*) and concentrated in ISG and not present in a post-ISG fraction obtained by centrifuging the 20,800 × *g* supernatant fraction at 130,000 × *g* for 1 h to obtain a pellet enriched in plasma membrane, microsomes, and trans-Golgi network and designated 21K-130K These samples are from the same preparation as shown in Fig. 5*C*. *C*, the level of ATP8B1 is high in human islets. *D*, ATP8B1 is concentrated in ISG purified by subcellular centrifugation alone or further purification with sucrose or Nycodenz gradients of the ISG obtained by subcellular centrifugation. An ATP8B1 knockdown cell line (ATP8B1 127-1) shows lower ATP8B1 protein levels in whole cell homogenate and ISG compared with the control cell line (pHygC) that shows the endogenous levels.

schemes used to obtain ISG. This resulted in a slight contamination of mitochondria with ISG. An immunoblot with an antibody against VAMP2, a marker for ISG, showed that the ISG fraction used contains a high concentration of this marker and no mitochondrial glycerol phosphate dehydrogenase enzyme activity in the ISG fraction (Fig. 2). Mitochondrial glycerol phosphate dehydrogenase is present only in mitochondria, and its concentration in beta cell mitochondria is among the highest in the body, making it an exceptionally sensitive marker for mitochondria in beta cells (51). Thus, although the mitochondrial fraction used was slightly contaminated with ISG, the ISG were not contaminated with mitochondria. The ISG fraction obtained by differential centrifugation was in some cases further purified by sucrose or Nycodenz gradient centrifugation to remove the slight contamination of peroxisomes in the ISG fraction (Fig. 3). We also further purified the light density fraction obtained by differential centrifugation using sucrose gradient centrifugation because of the high concentration of PS in the plasma membrane of most types of cells and the known presence of certain P4 ATPases in the plasma membrane and the trans-Golgi network known to be present in the light density subcellular fraction of the cell.

Immunoblot analysis was used to estimate the relative levels of the proteins, the catalytic units of the P4 ATPases. This showed very high levels of ATP8B1 protein in human pancreatic islets (Fig. 4*C*) and that in INS-1 832/13 cells ATP8B1 concentrated in ISG purified by differential centrifugation alone (Fig. 4, *A* and *B*) or in ISG further purified by sucrose or Nycodenz gradient centrifugation compared with a homogenate of whole cells (Fig. 4*D*). ATP8B1 appears as a broad band in immunoblots because it exists in multiple glycosylated and unglycosylated forms. In the immunoblots, the intensity of the ATP8B1 protein band in ISG samples at an equal or lower protein applied per lane was much darker than those of homogenates of whole cells or other subcellular fractions, such as mitochondria or plasma membrane (Fig. 4, *A*, *B*, and *D*), indicating that ATP8B1 is concentrated in ISG. In addition, mass spectrometry protein analysis of very pure (purified by differential centrifugation followed by centrifugation on a sucrose gradient) ISG from INS-1 832/13 cells showed that ATP8B1 is present in ISG. Another indication of the high level of localization of ATP8B1 to ISG was that knockdown of ATP8B1 in INS-1 832/13 cells severely lowered the ATP8B1 protein in ISG (cell line ATP8B1 127-1 in Fig. 4*D*). ATP8B1 was not present in a low

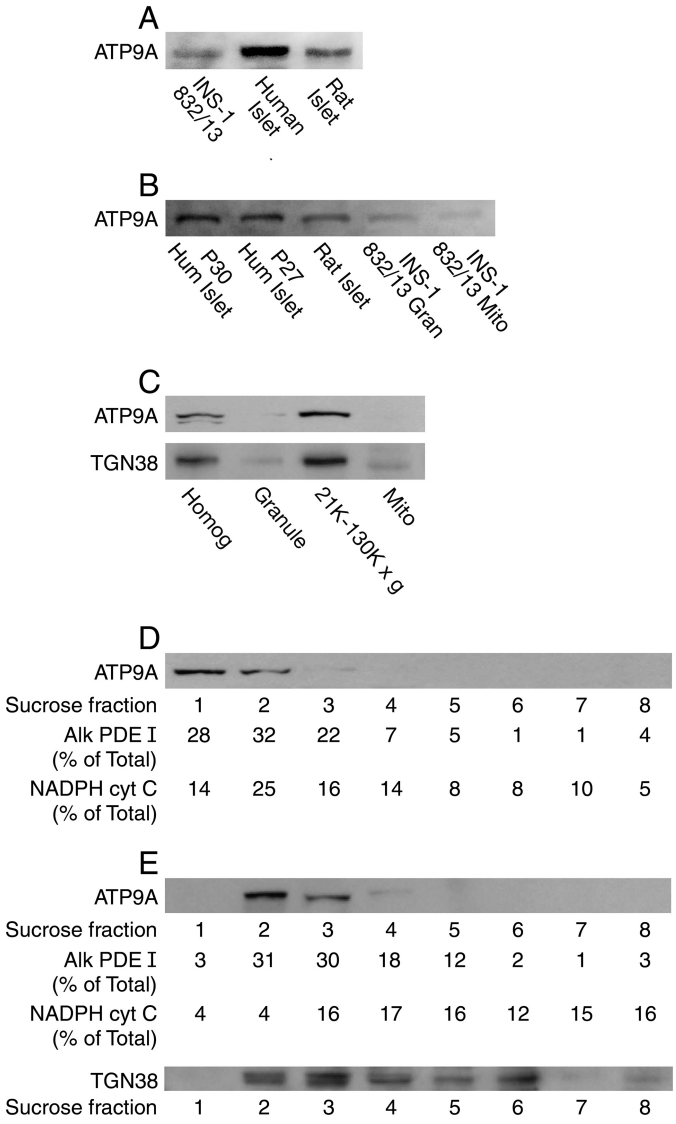

FIGURE 5. **ATP9A protein is highly expressed in human and rat pancreatic islets and at moderate levels in INS-1 832/13 cells, and in INS-1 832/13 cells, it is concentrated in plasma membrane and possibly the trans-Golgi network.** *A*, immunoblot with 20 μg of protein/lane. *B*, immunoblot with 20 μg of protein/lane. P30 and P27 are human pancreatic islets from two different donors. *C*, ATP9A is present in a homogenate of whole INS-1 832/13 cells (*Homog*) and at a low concentration or absent in ISG and is absent in mitochondria (*Mito*) and is concentrated in a post-ISG fraction obtained by centrifuging the 20,800 $\times$ *g* supernatant fraction at 130,000 $\times$ *g* for 1 h to obtain a pellet enriched in plasma membrane, microsomes (as shown in *D*), and the trans-Golgi network (as shown by the immunoblot of the trans-Golgi network marker shown as TGN38 in *C*) and designated 21K-130K x g. Samples in *C* are from the same preparations shown in Fig. 4*B*. *D*, ATP9A is concentrated in the plasma membrane. The figure shows an immunoblot of equal volume of each sucrose gradient fraction/lane along with percentages of the total sum of the enzyme activities of markers for plasma membrane (alkaline phosphodiesterase I (*Alk PDE I*)) and the microsomal fraction (NADPH cytochrome *c* reductase) across the sucrose fractions. A 35K-130K x g pellet enriched in plasma membrane was further purified by sucrose density gradient centrifugation. The post-20,800 $\times$ *g* ISG pellet, as in Fig. 4*C*, was centrifuged at 35,000 $\times$ *g* for 10 min, and the resulting supernatant fraction was centrifuged at 130,000 $\times$ *g* for 1 h to generate a pellet that was resuspended and layered on top of a sucrose gradient as described under "Experimental Procedures." The *lowest* to *highest numbers* indicate the lowest to highest density sucrose fractions. The levels of ATP9A in the immunoblot correspond more closely to the distribution of the enzyme activity of the plasma membrane marker enzyme alkaline phosphodiesterase I than to the distribution of the enzyme activity of the microsomal fraction (that also contains endoplasmic reticulum) marker enzyme NADPH cytochrome *c* reductase. *E*, ATP9A is concentrated in plasma membrane and in addition possibly in the trans-Golgi network. The figure shows an immunoblot of equal volume of each sucrose gradient fraction/lane from a post-nuclei/cell debris (600 $\times$ *g* for 10 min) supernatant fraction (*i.e.* not prepurified by subcellular centrifugation as in *C* or *D*) applied to a sucrose gradient and centrifuged at 100,00 $\times$ *g* for 3 h. The distribution of ATP9A again corresponds most closely to that of the plasma membrane marker alkaline phosphodiesterase I than to the microsomal marker NADPH cytochrome *c* reductase, which would also represent densities of the endoplasmic reticulum and trans-Golgi network. However, the distribution of the specific trans-Golgi network marker TGN38 (trans-Golgi network protein), although more broad than the distribution of ATP9A and the plasma membrane marker, significantly overlaps with the distribution of ATP9A, possibly indicating the presence of ATP9A in the trans-Golgi network.

density plasma membrane/microsome pellet/trans-Golgi network fraction of INS-1 832/13 cells obtained by centrifuging the post-ISG (20,800 $\times$ *g*) supernatant fraction at 130,000 $\times$ *g* (labeled *21K-130K* in Fig. 4*B*).

Immunoblot analysis showed a high level of ATP9A protein in human and rat pancreatic islets and a moderate amount in INS-1 832/13 cells (Fig. 5, *A*–*C*). Although mass spectrometry proteomics analysis of very pure ISG from INS-1 832/13 cells showed that ATP9A is present in ISG, immunoblot analysis showed that the level of ATP9A in ISG is low (Fig. 5, *B* and *C*). In contrast, immunoblot analysis of the INS-1 832/13 light density cell pellet obtained by centrifuging the post-ISG (20,800 $\times$ *g* for 20 min) supernatant fraction at 130,000 $\times$ *g* for 1 h (labeled *21K-130K* in Fig. 5*C*) (which was the very same crude plasma membrane pellet preparation that showed that ATP8B1 is absent in this subcellular fraction (Fig. 4*B*)) showed that ATP9A is concentrated in the plasma membrane or trans-Golgi network (Fig. 5*C*). This light membrane fraction was further purified by sucrose gradient centrifugation to attempt to separate the plasma membrane from the microsomal fraction that would contain trans-Golgi network and endoplasmic reticulum membranes in addition to microsome membranes. The post-ISG (20,800 $\times$ *g* for 20 min) supernatant fraction was centrifuged at 35,000 $\times$ *g*, and the resulting supernatant fraction was centrifuged at 130,000 $\times$ *g* to generate a pellet. This 35K-130K pellet was resuspended in KMSH solution and further purified by sucrose gradient centrifugation. Immunoblot analysis of the gradient fractions showed that the low density sucrose fractions of 10 and 20% contained the highest amount of ATP9A (Fig. 5*D*). This distribution of ATP9A across the lower density sucrose gradient fractions corresponded more closely to the distribution of the plasma membrane marker alkaline phosphodiesterase I than to the microsomal marker NADPH cytochrome *c* reductase that was distributed more broadly across all of the sucrose fractions (Fig. 5*D*), suggesting that ATP9A was concentrated in the plasma membrane. In addition to microsomes, the "microsomal" fraction contains organelles of similar density to microsomes, such as endoplasmic reticulum and the trans-Golgi network. To attempt two discern whether ATP9A is present in the trans-Golgi network (where it has been reported to be present in non-beta cells (52)) in addition to in the plasma membrane, a 600 $\times$ *g* supernatant fraction of INS-1 832/13 cells was further purified with sucrose gradient centrifugation (Fig. 5*E*). This showed that the distribution of ATP9A across the sucrose gradient fractions coincided more closely with the distribution of plasma membrane marker than the trans-Golgi network marker TGN38. The distribution of TGN38 closely overlapped with the distribution of ATP9A and the plasma

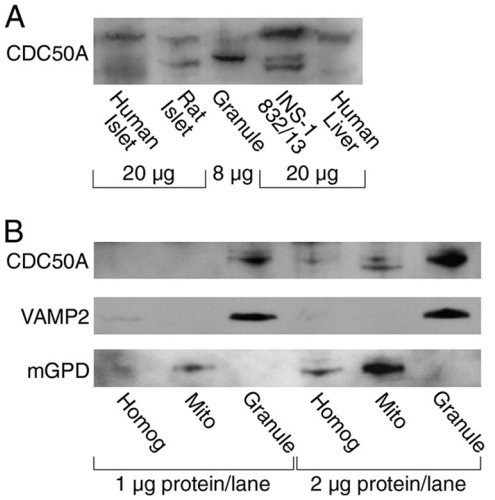

FIGURE 6. **CDC50A protein is present in human and rat pancreatic islets and INS-1 832/13 cells and is concentrated in insulin secretory granules of beta cells.** *A*, immunoblot with 8 or 20 μg of protein/lane showing the presence of CDC50A in human and rat pancreatic islets as well as in INS-1 832/13 cells and ISG of INS-1 832/13 cells. CDC50A appears as multiple bands due to glycosylated and unglycosylated forms. *B*, CDC50A is concentrated in insulin secretory granules of beta cells. Shown is an immunoblot of insulin secretory granules, a whole cell homogenate (*Homog*), and mitochondria (*Mito*) from INS-1 832/13 cells with very low amounts of protein per lane. VAMP2 and mitochondrial glycerol phosphate dehydrogenase (*mGPD*) are markers of ISG and mitochondria, respectively. All or most of the CDC50A in mitochondria is probably attributable to contamination from ISG in this fraction from the subcellular purification scheme that was purposely designed to obtain ISG free of mitochondria but not *vice versa* (see "Experimental Procedures").

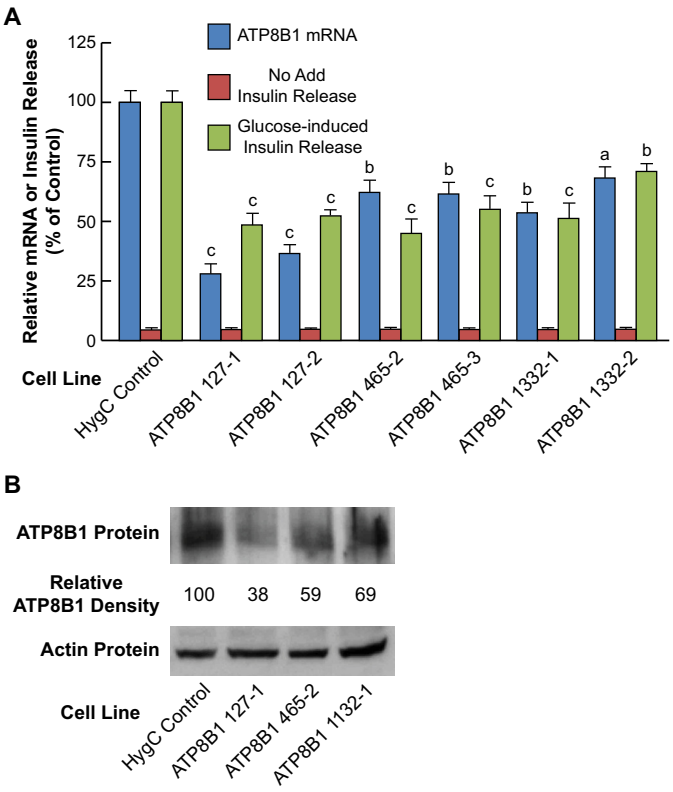

FIGURE 7. **Knockdown of *Atp8b1* mRNA and ATP9A protein inhibits glucose-induced insulin release in INS-1 832/13 cells.** Glucose-induced insulin release of the HygC nontargeting shRNA cell line is expressed as 100% and equals 16.3 ± 0.9 milliunits of insulin/mg of whole cell protein/1 h. Results are the means ± S.E. (*error bars*) for mRNA measurements on three separate cell preparations and insulin release on 12 or more replicate incubations. *a*, $p < 0.02$; *b*, $p < 0.01$; *c*, $p < 0.001$ *versus* the same condition for the control. *B*, immunoblot with 15 μg of protein/lane with anti-ATP8B1 antibody showing that the relative density of the targeted cell line is decreased compared with the HygC non-targeting shRNA cell line and with the immunoblot membrane reprobed with anti-beta actin antibody to show equal loading of protein across lanes.

membrane marker alkaline phosphodiesterase I, but TGN38 was distributed across a broader range of fractions than the plasma membrane marker alkaline phosphodiesterase I and ATP9A. This suggests that although ATP9A is concentrated in the plasma membrane, it might also be present in the trans-Golgi network.

ATP8B2 protein was not analyzed by immunoblotting because we were unable to acquire an antibody satisfactory for detection of the protein (two different antibodies were tried) even in the liver, where it is known to be present. However, *Atp8b2* mRNA was plentiful in INS-1 832/13 cells, as mentioned above, and knockdown of its mRNA inhibited glucose-stimulated insulin release (see below).

CDC50A has been localized with immunocytochemistry to granules in the pancreas and was seen in both exocrine and endocrine cells of the pancreas (29). Immunoblot analysis showed that CDC50A is expressed in INS-1 832/13 cells as well as in human and rat pancreatic islets (Fig. 6*A*). The concentration of CDC50A is very high in ISG in INS-1 832/13 cells, as judged from its easy detection with as little as 1 μg of ISG protein/lane in immunoblots (Fig. 6*B*). CDC50A appears as multiple bands in immunoblots because it is present in glycosylated and unglycosylated forms (29) (Fig. 4, *A* and *B*).

Knockdown of Atp8b1, Atp8b2, Atp9a, and Cdc50a Expression in Pure Beta Cells Inhibits Glucose-stimulated Insulin Release—Stable transfection of shRNA was used to generate multiple INS-1 832/13-derived knockdown cell lines for ATP8B1, ATP8B2, ATP9A, and CDC50A with various levels of knockdown of each enzyme. As we have often observed in previous similar studies when using multiple cell lines showing various levels of knockdown of a single enzyme, the order of knockdown among cell lines was roughly as follows: decrease of mRNA > decrease of protein > inhibition of insulin release (53). Among cell lines with the same gene targeted, glucose-induced insulin release was inhibited roughly in proportion to the knockdown of the P4 ATPase mRNAs and proteins. Knockdown of *Atp8b1* mRNA varied between 45 and 73% (Fig. 7*A*) and was associated with 31–62% decreases in ATP8B1 protein levels in whole cells (Fig. 7*B*), about 85% knockdown of ATP8B1 protein in ISG (Fig. 4*D*), and 40–67% decreases in glucose-stimulated insulin release (Fig. 7*A*). *Atp8b2* mRNA knockdown varied between 23 and 77%, and glucose-stimulated insulin release was inhibited fairly proportionate to mRNA knockdown, with decreases of 25–45% in glucose-stimulated insulin release in three of the four ATP8B2 knockdown cell lines (Fig. 8). Knockdown of *Atp9a* mRNA 95% (Fig. 9, *top*) was associated with 52–77% knockdown of ATP9A protein (Fig. 9, *bottom*) and 45–63% inhibition of glucose-stimulated insulin release (Fig. 9, *top*). Stable knockdown of *Cdc50a* mRNA varied between 45 and 80% in INS-1 832/13 cells (Fig. 10*A*) and was associated with 19–85% knockdown of CDC50A protein (Fig. 10*B*) and 33–57% inhibition of glucose-stimulated insulin release (Fig. 10*A*).

The levels of the mRNAs that encode ATP9B and ATP11B in INS-1 832/13 cells, human pancreatic islets, and rat pancreatic

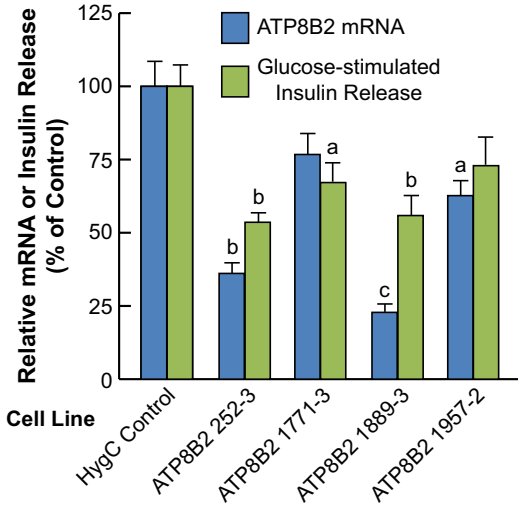

FIGURE 8. **Knockdown of *Atp8b2* mRNA inhibits glucose-induced insulin release in INS-1 832/13 cells.** Glucose-induced insulin release of the HygC nontargeting shRNA cell line is expressed as 100% and equals 18.2 ± 1.2 milliunits of insulin/mg of whole cell protein/1 h. Results are the means ± S.E. (*error bars*) for mRNA measurements on three separate cell preparations and insulin release on 16 or more replicate incubations. *a*, $p < 0.05$; *b*, $p < 0.01$; *c*, $p < 0.001$ *versus* the same condition for the control.

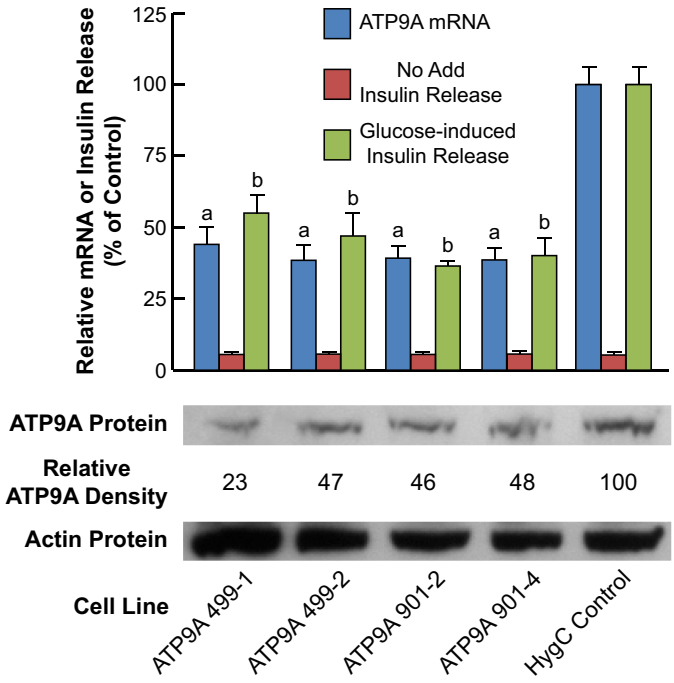

FIGURE 9. **Knockdown of *Atp9a* mRNA and ATP9A protein inhibits glucose-induced insulin release in INS-1 832/13 cells.** *Top*, glucose-induced insulin release of the HygC nontargeting shRNA cell line expressed as 100% (100% equaled 17.3 ± 1.0 milliunits of insulin/mg of whole cell protein/1 h). Results are the means ± S.E. (*error bars*) for mRNA measurements on three separate cell preparations and insulin release on 12 or more replicate incubations. *a*, $p < 0.01$; *b*, $p < 0.001$ *versus* the same condition for the control. *Bottom*, immunoblot with 30 μg of cell protein/lane with anti-ATP9A antibody and with density of ATP9A bands relative to that in the HygC nontargeting shRNA cell line and with the immunoblot membrane reprobed with anti-beta actin antibody to show equal loading of protein across lanes.

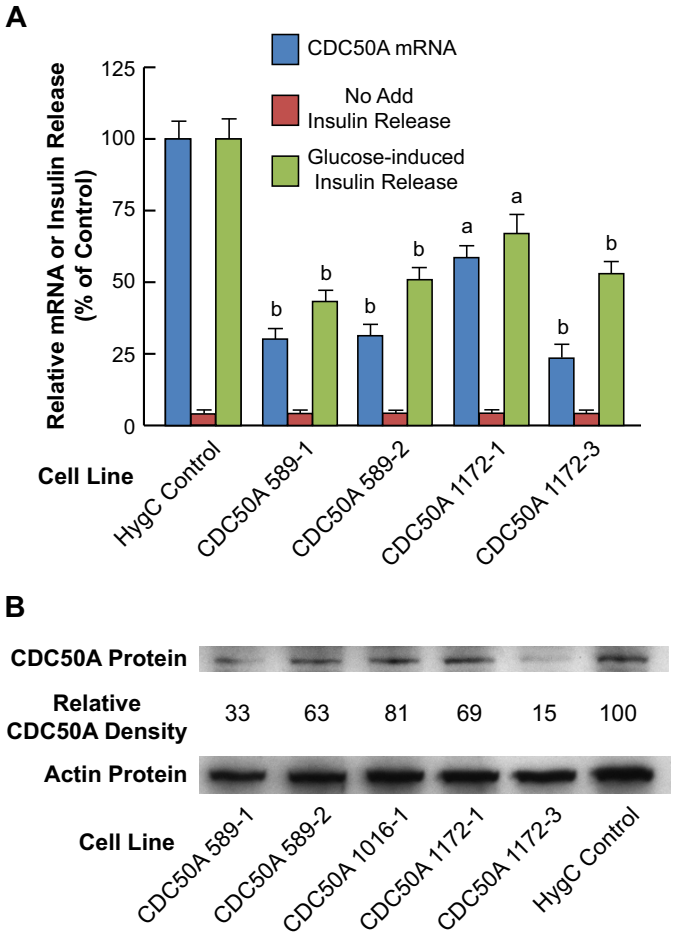

FIGURE 10. **Knockdown of *Cdc50a* mRNA and CDC50A protein correlates with inhibition of glucose-induced insulin release in INS-1 832/13 cells.** Glucose-induced insulin release of the HygC nontargeting shRNA cell line is expressed as 100% and equals 16 ± 1.1 milliunits of insulin/mg of whole cell protein/1 h. Results are the means ± S.E. (*error bars*) for mRNA measurements on three separate cell preparations and insulin release on 12 or more replicate incubations. *a*, $p < 0.01$; b, $p < 0.001$ *versus* the same condition for the control. *B*, immunoblot with 18 μg of protein/lane with anti-CDC50A antibody and showing decreased density of CDC50A bands of targeted cell lines relative to the HygC non-targeting shRNA cell line and with the immunoblot membrane reprobed with anti-beta actin to show equal loading of protein across lanes.

islets were very low compared with the levels of mRNAs that encode ATP8B1, ATP8B2, ATP9A, and CDC50A, but the levels of *Atp9b* and *Atp11b* mRNAs were above the limit of detection (Fig. 1). As an additional control to test the relevance of the above highly expressed proteins in insulin secretion, INS-1 832/13-derived cell lines with stably knocked down *Atp9b* and *Atp11b* mRNAs were generated. *Atp9b* mRNA knockdown varied between 50 and 66% in four cell lines, and ATP11B mRNA knockdown varied between 53 and 71% in six cell lines. Glucose-stimulated insulin release in these cell lines was similar to the glucose-stimulated insulin release of the control cell lines (data not shown), indicating that, in contrast to the more highly expressed P4 ATPases, these two P4 ATPases expressed at a low level in beta cells do not seem to be essential for insulin secretion.

Knockdown of Atp8b1, Atp9a, and Cdc50a Expression in Beta Cells Inhibits BCH plus Glutamine-stimulated Insulin Release—Dhar *et al.* (54) have suggested that loss of ATP10A, a P4 ATPase (that was not a P4 ATPase identified in beta cells in our study) in adipose and skeletal muscle in a mouse model of type 2 diabetes causes insulin resistance by interfering with the normal insulin-stimulated translocation of GLUT4 to the

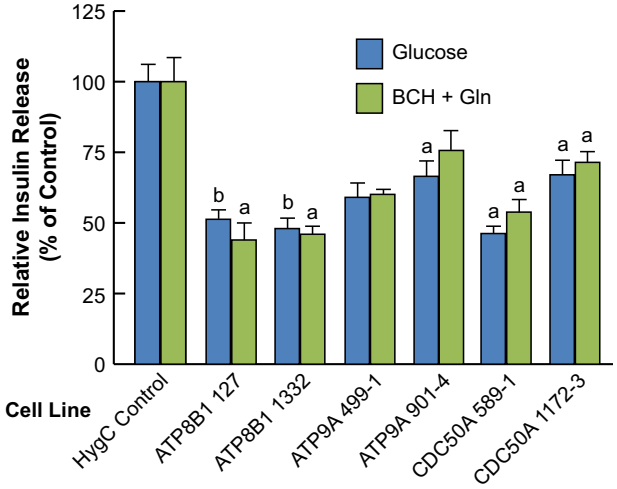

FIGURE 11. **Knockdown of BCH plus glutamine-stimulated insulin release is similar to knockdown of glucose-stimulated insulin release in ATP8B1, ATP9A, or CDC50A knockdown cell lines.** Insulin release stimulated by BCH (10 mM) plus glutamine (10 mM) was compared with glucose (11.1 mM)-stimulated insulin release in INS-1 832/13 cell lines with knockdown of *Atp8b1*, *Atp9a*, or *Cdc50a* expression as described under "Experimental Procedures." Results are the means ± S.E. (*error bars*) for eight replicate incubations for each cell line and each condition. Insulin releases in the pHygC control cell line in the presence of glucose and of BCH plus glutamine expressed as 100% were 17.5 ± 0.9 and 26.6 ± 1.6 milliunits/mg of whole cell protein/1 h, respectively. *a*, $p < 0.01$; *b*, $p < 0.001$ *versus* control cell line with the same stimulant.

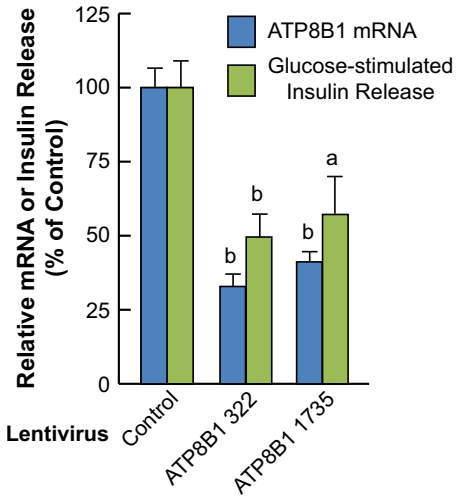

FIGURE 12. **Knockdown of *ATP8B1* expression in human pancreatic islets inhibits glucose-induced insulin release.** Human pancreatic islets were infected with lentivirus containing shRNAs targeting *ATP8B1* or a scrambled DNA sequence as a control. Insulin release and mRNA measurements were as described under "Experimental Procedures." Results are expressed as a percentage of glucose-stimulated insulin release minus unstimulated (no secretagogue added) insulin release compared with the control value. mRNA values are the mean ± S.E. (*error bars*) of three replicate measurements for each condition. Insulin release measurements are the mean ± S.E. of 12–18 replicate incubations from two or three separate islet preparations. *a*, $p < 0.05$; *b*, $p < 0.001$ *versus* control.

plasma membrane, resulting in decreased glucose uptake in adipose tissue and skeletal muscle. To show that decreased glucose transport into beta cells was probably not the cause of inhibited glucose-stimulated insulin release in our P4 ATPase knockdown cell lines, we studied insulin release stimulated by BCH plus glutamine, a potent non-glucose stimulus of insulin release in pancreatic beta cells. Fig. 11 shows that the inhibition of BCH plus glutamine-stimulated insulin release in the INS-1 8321/3-derived cell lines with knockdown of *Atp8b1*, *Atp9a*, and *Cdc50a* was similar to the inhibition of glucose-stimulated insulin release. This result indicates that, as we expected, the inhibition of glucose-stimulated insulin release was not due to diminished glucose transport into these cells but rather due to inhibition of the rapid translocation of PS and PE from the luminal leaflet of the ISG lipid bilayer to the cytosolic leaflet of the ISG lipid bilayer and possibly also inhibition of translocation of these phospholipids in the plasma membrane to its cytosolic leaflet.

Knockdown of ATP8B1, ATP9A, and CDC50A Expression in Human Pancreatic Islets Inhibits Glucose-stimulated Insulin Release—Human pancreatic islets were transiently infected with lentiviruses containing vectors that targeted two independent locations in mRNAs of *ATP8B1*, *ATP9A*, and *CDC50A* in order to study their effect on glucose-stimulated insulin release. Glucose-stimulated insulin release was inhibited roughly in proportion to the knockdown of mRNA in the human pancreatic islets. *ATP8B1* mRNA was decreased 67 and 59%, and glucose-stimulated insulin release was inhibited 50 and 43% (Fig. 12). *ATP9A* mRNA was lowered 52 and 46%, and glucose-stimulated insulin release was inhibited 32 and 47% (Fig. 13). *CDC50A* mRNA was decreased 82 and 72%, and glucose-stimulated insulin release was inhibited 65 and 70%, respectively (Fig. 14).

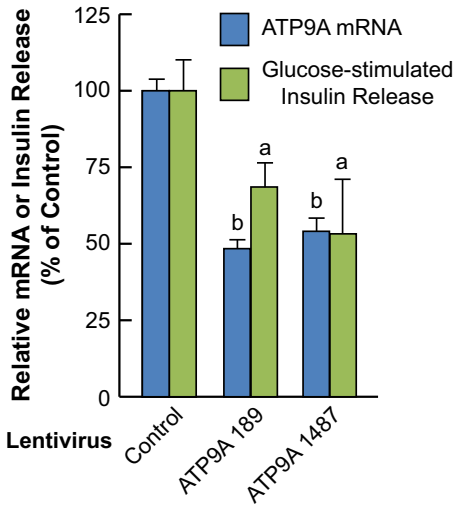

FIGURE 13. **Knockdown of *ATP9A* expression in human pancreatic islets inhibits glucose-induced insulin release.** Human pancreatic islets were infected with Lentivirus containing shRNAs targeting *ATP9A* or a scrambled DNA sequence as a control. Conditions were the same as in Fig. 12. *a*, $p < 0.05$; *b*, $p < 0.001$ *versus* control. *Error bars*, S.E.

Discussion

P4 ATPase flippase enzymes move PS and to a lesser extent PE to the cytoplasmic leaflets of secretory vesicles and plasma membrane over a time frame of seconds. The inhibition of secretagogue-stimulated insulin release in pure beta cells (Figs. 7, 8, 9, and 11) and human pancreatic islets (Figs. 12 and 13) with knocked down ATP8B1, ATP8B2, or ATP9A along with the identification of ATP8B1 in ISG (Fig. 4) and ATP9A in the plasma membrane (Fig. 5) further support the idea that ISG PS is important for generating fusion-competent lipid membranes in insulin secretion. The negative charge of PS acts as a coupling

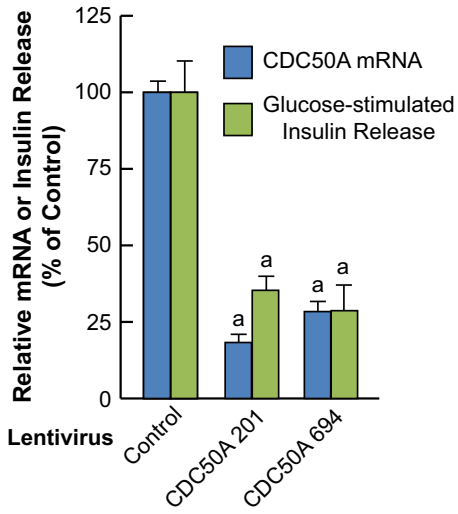

FIGURE 14. **Knockdown of *CDC50A* expression in human pancreatic islets inhibits glucose-induced insulin release.** Human pancreatic islets were infected with Lentivirus containing shRNAs targeting *CDC50A* or a scrambled DNA sequence as a control. Conditions were the same as in Fig. 12. *a*, $p < 0.001$ *versus* control. *Error bars*, S.E.

factor to facilitate the zippering interaction between the domains of positively charged amino acids of secretory vesicle SNARE proteins with similar domains of positively charged amino acids in the plasma membrane SNARE proteins in secretory cells (2–7). Our earlier paper (1) showed that PS is concentrated in ISG and increases in ISG with glucose stimulation. In most types of cells, the plasma membrane is known to contain a high concentration of PS.

Differential centrifugation alone generates >90% pure ISG, and further purification of this ISG fraction with gradient centrifugation yields very pure ISG. The identification of ATP8B1 in ISG purified by differential centrifugation alone (Fig. 4, *A* and *B*) and further purified by sucrose gradient centrifugation (Fig. 4*D*) as well as the targeted knockdown of ATP8B1 in INS-1 832/13 cells severely lowering ATP8B1 in ISG (Fig. 4*D*) unequivocally shows that ATP8B1 is concentrated in ISG. ATP8B1 and ATP8B2 are present in intracellular vesicles in many human tissues (27). P4 ATPase flippase enzymes are also present in the plasma membranes and trans-Golgi network of many cells. We found ATP9A to be present at a very low concentration in ISG (Fig. 5, *B* and *C*). Although we also found ATP9A in very pure ISG with mass spectrometry analysis, it is possible that the low concentration in ISG is from contamination from another subcellular fraction(s). ATP9A is present at a very high concentration in a plasma membrane/trans-Golgi network subcellular fraction (labeled *21K-130K x g* in Fig. 5*C*). Unlike with ISG, pure plasma membrane and pure trans-Golgi network cannot be obtained by differential centrifugation alone. When a light density (*35K-130K x g*) subcellular fraction was further purified by centrifugation on a sucrose gradient, there was overlap in gradient fractions containing plasma membrane and microsomal marker enzymes (Fig. 5*D*). However, the distribution of ATP9A across the lighter density sucrose gradient fractions correlated more closely with the plasma membrane marker alkaline phosphdiesterase I than with the distribution of the microsomal marker NADPH cytochrome *c* reductase that was broadly distributed across the gradient (Fig. 5*D*), suggesting that ATP9A was concentrated in the plasma membrane. In addition to microsomes, the "microsomal" fraction contains organelles of similar density to microsomes, such as endoplasmic reticulum and the trans-Golgi network. To attempt to discern whether ATP9A is present in the trans-Golgi network in addition to or instead of in the plasma membrane, a 600 × *g* supernatant fraction of INS-1 832/13 cells was further purified with sucrose gradient centrifugation (Fig. 5*E*). This also showed that the distribution of ATP9A across the sucrose gradient fractions corresponded more closely to the plasma membrane marker than to the trans-Golgi network marker TGN38 that was distributed across a broader range of fractions than ATP9A and the plasma membrane marker alkaline phosphodiesterase I (Fig. 5*E*), suggesting that ATP9A was present in plasma membrane but possibly also concentrated in the trans-Golgi network. A presence of ATP9A in the trans-Golgi network would suggest that the enzyme is important for vesicle biogenesis (8). ATP9A is present in the trans-Golgi network in yeast (52), where it is believed to play a role in vesicle biogenesis. In the plasma membrane, the main function of a P4 ATPase is to move PS to the cytoplasmic leaflet of the membrane. This would facilitate the docking interaction between the ISG membrane and the plasma membrane, as mentioned above. Taken together, the current data combined with recent data that showed that PS is concentrated in ISG (1) further suggest that PS and its increase in beta cells (55) with glucose stimulation (1) is important for insulin secretion.

CDC50A has been shown by immunohistochemistry to be present in granules in both exocrine and endocrine cells of the pancreas (29). CDC50A functions as a subunit of P4 ATPases that upon heterodimerization with P4 ATPases forms a phospholipid translocation complex (26–30). We found very high levels of CDC50A in ISG that was easily detectable with very low levels of ISG protein per lane in immunoblot analyses (Fig. 6, *A* and *B*). It was therefore not surprising that knockdown of CDC50A with shRNA technology in INS-1 832/13 cells (Fig. 10) and human pancreatic islets (Fig. 14) inhibited glucose-stimulated insulin release.

Conclusion

Recent data have shown that PS is concentrated in beta cell ISG 5-fold compared with the whole beta cell and increases in ISG with glucose stimulation (1). The current results show that knockdown of highly expressed P4 ATPases and CDC50A in pure beta cells and human pancreatic islets (Figs. 4–6) that are concentrated in ISG (ATP8B1 and CDC50A) or in the plasma membrane and possibly the trans-Golgi network (ATP9A) inhibits secretagogue-stimulated insulin release in these cells (Figs. 7–14). The presence of ATP9A in the trans-Golgi network implicates this P4 ATPase in vesicle biogenesis. The PS data (1, 55) combined with the current flippase data suggest that the inhibition of stimulated-insulin release is due to inhibition of translocation of PS to the cytosolic leaflets of the ISG and plasma membrane lipid bilayers, where the negatively charged PS acts as a coupling factor enhancing the zippering-like fusion of the positively charged amino acid domains of secretory vesicle SNARE proteins and the positively charged

amino acid domains of the plasma membrane SNARE proteins (2–7). The inhibition of this translocation should inhibit the docking and fusion of the ISG with the plasma membrane during insulin exocytosis and would inhibit glucose-stimulated insulin release. Inhibition of normal vesicle biogenesis by knockdown of a P4 ATPase located in the trans-Golgi network could also contribute to inhibition of stimulated insulin release.

PS on the cytosolic leaflet of vesicles and the plasma membrane could play additional roles that facilitate their docking with plasma membrane proteins with specific PS-binding domains. The synaptic vesicle protein synaptotagmin 1 (Syt1) binds PS in a calcium-dependent manner (18, 19). It has been shown that increased PS levels in PC12 cells produce an increase in calcium-triggered membrane fusion and exocytosis and catecholamine release (16, 17). PS may also play a role in membrane curvature that increases membrane fusion and exocytosis of proteins. Several naturally occurring proteins can sense membrane curvature. A 25-mer peptide, MARCKS-ED, based on the effector domain sequence of the intracellular membrane protein myristoylated alanine-rich protein kinase C substrate can recognize PS with preferences for highly curved vesicles (20).

Author Contributions—I. H. A. designed and executed experiments and contributed to writing the manuscript. C. C. P. contributed to the design of experiments and writing of the manuscript. M. J. L. contributed to the design of experiments and executed experiments. M. A. K. and S. W. S. executed experiments. M. J. M. designed experiments and wrote the manuscript. All authors analyzed the results and approved the final version of the manuscript.

References

1. MacDonald, M. J., Ade, L., Ntambi, J. M., Ansari, I. H., and Stoker, S. W. (2015) Characterization of phospholipids in insulin secretory granules in pancreatic beta cells and their changes with glucose stimulation. *J. Biol. Chem.* **290,** 11075–11092
2. Yeung, T., Gilbert, G. E., Shi, J., Silvius, J., Kapus, A., and Grinstein, S. (2008) Membrane phosphatidylserine regulates surface charge and protein localization. *Science* **319,** 210–213
3. Williams, D., Vicôgne, J., Zaitseva, I., McLaughlin, S., and Pessin, J. E. (2009) Evidence that electrostatic interactions between vesicle-associated membrane protein 2 and acidic phospholipids may modulate the fusion of transport vesicles with the plasma membrane. *Mol. Biol. Cell* **20,** 4910–4919
4. de Haro, L., Ferracci, G., Opi, S., Iborra, C., Quetglas, S., Miquelis, R., Lévèque, and Seagar, M. (2004) Ca^{2+}/calmodulin transfers the membrane-proximal lipid-binding domain of the v-SNARE synaptobrevin from cis to trans bilayers. *Proc. Natl. Acad. Sci. U.S.A.* **101,** 1578–1583
5. Domanska, M. K., Kiessling, V., and Tamm, L. K. (2010) Docking and fast fusion of synaptobrevin vesicles depends on the lipid compositions of the vesicle and the acceptor SNARE complex-containing target membrane. *Biophys. J.* **99,** 2936–2946
6. Quetglas, S., Iborra, C., Sasakawa, N., De Haro, L., Kumakura, K., Sato, K., Leveque, C., and Seagar, M. (2002) Calmodulin and lipid binding to synaptobrevin regulates calcium-dependent exocytosis. *EMBO J.* **21,** 3970–3979
7. Kooijman, E. E., King, K. E., Gangoda, M., and Gericke, A. (2009) Ionization properties of phosphatidylinositol polyphosphates in mixed model membranes. *Biochemistry* **48,** 9360–9371
8. Folmer, D. E., Elferink, R. P., and Paulusma, C. C. (2009) P4 ATPases: lipid flippases and their role in disease. *Biochim. Biophys. Acta.* **1791,** 628–635
9. Daleke, D. L. (2007) Phospholipid flippases. *J. Biol. Chem.* **282,** 821–825
10. Devaux, P. F., Herrmann, A., Ohlwein, N., and Kozlov, M. M. (2008) How lipid flippases can modulate membrane structure. *Biochim. Biophys. Acta* **1778,** 1591–1600
11. Clark, M. R. (2011) Flippin' lipids. *Nat. Immunol.* **12,** 373–375
12. van Meer, G., Voelker, D. R., and Feigenson, G. W. (2008) Membrane lipids: where they are and how they behave. *Nat. Rev. Mol. Cell Biol.* **9,** 112–124
13. van der Mark, V. A., Elferink, R. P., and Paulusma, C. C. (2013) P4 ATPases: flippases in health and disease. *Int. J. Mol. Sci.* **14,** 7897–7922
14. Coleman, J. A., Quazi, F., and Molday, R. S. (2013) Mammalian P4-ATPases and ABC transporters and their role in phospholipid transport. *Biochim. Biophys. Acta* **1831,** 555–574
15. Leventis, P. A., and Grinstein, S. (2010) The distribution and function of phosphatidylserine in cellular membranes. *Annu. Rev. Biophys.* **39,** 407–427
16. Zhang, Z., Hui, E., Chapman, E. R., and Jackson, M. B. (2009) Phosphatidylserine regulation of Ca^{2+}-triggered exocytosis and fusion pores in PC12 cells. *Mol. Biol. Cell* **20,** 5086–5095
17. Lam, A. D., Tryoen-Toth, P., Tsai, B., Vitale, N., and Stuenkel, E. L. (2008) SNARE-catalyzed fusion events are regulated by syntaxin1A-lipid interactions. *Mol. Biol. Cell* **19,** 485–497
18. Jackson, M. B., and Chapman, E. R. (2006) Fusion pores and fusion machines in Ca^{2+}-triggered exocytosis. *Annu. Rev. Biophys. Biomol. Struct.* **35,** 135–160
19. Chapman, E. R. (2008) How does synaptotagmin trigger neurotransmitter release? *Annu. Rev. Biochem.* **77,** 615–641
20. Morton, L. A., Yang, H., Saludes, J. P., Fiorini, Z., Beninson, L., Chapman, E. R., Fleshner, M., Xue, D., and Yin, H. (2013) MARCKS-ED peptide as a curvature and lipid sensor. *ACS Chem. Biol.* **8,** 218–225
21. Vance, D. E., and Vance, J. E. (2008) Phospholipid biosynthesis in eukaryotes. in *Biochemistry of Lipids, Lipoproteins and Membranes*, 5th Ed. (Vance, D. E., and Vance, J. E., eds) pp. 213–244, Elsevier, Amsterdam
22. Vance, J. E., and Tasseva, G. (2013) Formation and function of phosphatidylserine and phosphatidylethanolamine in mammalian cells. *Biochim. Biophys. Acta* **1831,** 543–554
23. Zachowski, A., Henry, J. P., and Devaux, P. F. (1989) Control of transmembrane lipid asymmetry in chromaffin granules by an ATP-dependent protein. *Nature* **340,** 75–76
24. Ding, J., Wu, Z., Crider, B. P., Ma, Y., Li, X., Slaughter, C., Gong, L., and Xie, X. S. (2000) Identification and functional expression of four isoforms of ATPase II, the putative aminophospholipid translocase: effect of isoform variation on the ATPase activity and phospholipid specificity. *J. Biol. Chem.* **275,** 23378–23386
25. Tang, X., Halleck, M. S., Schlegel, R. A., and Williamson, P. (1996) A subfamily of P-type ATPases with aminophospholipid transporting activity 1. *Science* **272,** 1495–1497
26. Paulusma, C. C., Folmer, D. E., Ho-Mok, K. S., de Waart, D. R., Hilarius, P. M., Verhoeven, A. J., and Oude Elferink, R. P. (2008) ATP8B1 requires an accessory protein for endoplasmic reticulum exit and plasma membrane lipid flippase activity. *Hepatology* **47,** 268–278
27. van der Velden, L. M., Wichers, C. G., van Breevoort, A. E., Coleman, J. A., Molday, R. S., Berger, R., Klomp, L. W., and van de Graaf, S. F. (2010) Heteromeric interactions required for abundance and subcellular localization of human CDC50 proteins and class 1 P4-ATPases. *J. Biol. Chem.* **285,** 40088–40096
28. Jacquot, A., Montigny, C., Hennrich, H., Barry, R., le Maire, M., Jaxel, C., Holthuis, J., Champeil, P., and Lenoir, G. (2012) Phosphatidylserine stimulation of Drs2p·Cdc50p lipid translocase dephosphorylation is controlled by phosphatidylinositol-4-phosphate. *J. Biol. Chem.* **287,** 44580
29. Folmer, D. E., Mok, K. S., de Wee, S. W., Duijst, S., Hiralall, J. K., Seppen, J., Oude Elferink, R. P. J., and Paulusma, C. C. (2012) Cellular localization and biochemical analysis of mammalian CDC50A, a glycosylated β-subunit for P4 ATPases. *J. Histochem. Cytochem.* **60,** 205–218
30. Coleman, J. A., and Molday, R. S. (2011) Critical role of the beta-subunit CDC50A in the stable expression, assembly, subcellular localization, and lipid transport activity of the P4-ATPase ATP8A2. *J. Biol. Chem.* **286,** 17205–17216
31. Hohmeier, H. E., Mulder, H., Chen, G., Henkel-Rieger, R., Prentki, M., and

Newgard, C. B. (2000) Isolation of INS-1-derived cell lines with robust ATP-sensitive K^+ channel-dependent and -independent glucose-stimulated insulin secretion. *Diabetes* **49,** 424–430
32. Brown, L. J., Longacre, M. J., Hasan, N. M., Kendrick, M. A., Stoker, S. W., and Macdonald, M. J. (2009) Chronic reduction of the cytosolic or mitochondrial NAD(P)P-malic enzyme does not affect insulin secretion in a rat insulinoma cell line. *J. Biol. Chem.* **284,** 35359–35367
33. MacDonald, M. J., Smith, A. D., 3rd, Hasan, N. M., Sabat, G., and Fahien, L. A. (2007) Feasibility of pathways for transfer of acyl groups from mitochondria to the cytosol to form short chain acyl CoAs in the pancreatic beta cell. *J. Biol. Chem.* **282,** 30596–30606
34. MacDonald, M. J., Longacre, M. J., Stoker, S. W., Kendrick, M., Thonpho, A., Brown, L. J., Hasan, N. M., Jitrapakdee, S., Fukao, T., Hanson, M. S., Fernandez, L. A., and Odorico, J. (2011) Differences between human and rodent pancreatic islets: low pyruvate carboxylase, ATP citrate lyase and pyruvate carboxylation; high glucose-stimulated acetoacetate in human pancreatic islets. *J. Biol. Chem.* **286,** 18383–18396
35. MacDonald, M. J. (1995) Feasibility of a mitochondrial pyruvate malate shuttle in pancreatic islets: further implication of cytosolic NADPH in insulin secretion. *J. Biol. Chem.* **270,** 20051–20058
36. MacDonald, M. J., Longacre, M. J., Langberg, E.-C., Tibell, A., Kendrick, M. A., Fukao, T., and Ostenson, C.-G. (2009) Decreased levels of metabolic enzymes in pancreatic islets of patients with type 2 diabetes. *Diabetologia* **52,** 1087–1091
37. Rana, R. S., Kowluru, A., and MacDonald, M. J. (1986) Secretagogue-responsive and -unresponsive pools of phosphatidylinositol in pancreatic islets. *Arch. Biochem. Biophys.* **245,** 411–416
38. Rana, R. S., Kowluru, A., and MacDonald, M. J. (1986) Enzymes of phospholipid metabolism in rat pancreatic islets: subcellular distribution and the effect of glucose and calcium. *J. Cell Biochem.* **32,** 143–150
39. Kowluru, A., Rana, R. S., and MacDonald, M. J. (1985) Phospholipid methyltransferase activity in pancreatic islets: activation by calcium. *Arch. Biochem. Biophys.* **242,** 72–81
40. Kowluru, A., Rabaglia, M. E., Muse, K. E., and Metz, S. A. (1994) Subcellular localization and kinetic characterization of guanine nucleotide binding proteins in normal rat and human pancreatic islets and transformed β cells. *Biochim. Biophys. Acta* **1222,** 348–359
41. Wang, Z., and Thurmond, D. C. (2010) Differential phosphorylation of RhoGDI mediates the distinct cycling of Cdc42 and Rac1 to regulate second-phase insulin secretion. *J. Biol. Chem.* **285,** 6186–6197
42. Spurlin, B. A., and Thurmond, D. C. (2006) Syntaxin 4 facilitates biphasic glucose-stimulated insulin secretion from pancreatic beta-cells. *Mol. Endocrinol.* **20,** 183–193
43. Rhodes, C. J., Brennan, S. O., and Hutton, J. C. (1989) Proalbumin to albumin conversion by a proinsulin processing endopeptidase of insulin secretory granules. *J. Biol. Chem.* **264,** 14240–14245
44. Brunner, Y., Couté, Y., Iezzi, M., Foti, M., Fukuda, M., Hochstrasser, D. F., Wollheim, C. B., and Sanchez, J. C. (2007) Proteomics analysis of insulin secretory granules. *Mol. Cell Proteomics* **6,** 1007–1017
45. Rana, R. S., and MacDonald, M. J. (1986) Phosphotidylinositol kinase in rat pancreatic islets: subcellular distribution and sensitivity to calcium. *Horm. Metab. Res.* **18,** 659–662
46. Aronson, N. N., Jr., and Touster, O. (1974) Isolation of rat liver plasma membrane fragments in isotonic sucrose. *Methods Enzymol.* **31,** 90–102
47. Masters, B. S. S., Williams, C. H., and Kamin, H. (1967) The preparation and properties of microsomal TPNH-cytochrome *c* reductase from pig liver. *Methods Enzymol.* **10,** 565–573
48. Rodrigues, R. B., Sabat, G., Minkoff, B. B., Burch, H. L., Nguyen, T. T., and Sussman, M. R. (2014) Expression of a translationally fused TAP-tagged plasma membrane proton pump in *Arabidopsis thaliana*. *Biochemistry* **53,** 566–578
49. Nesvizhskii, A. I., Keller, A., Kolker, E., and Aebersold, R. (2003) A statistical model for identifying proteins by tandem mass spectrometry. *Anal. Chem.* **75,** 4646–4658
50. Balciunas, D., Wangensteen, K. J., Wilber, A., Bell, J., Geurts, A., Sivasubbu, S., Wang, X., Hackett, P. B., Largaespada, D. A., McIvor, R. S., and Ekker, S. C. (2006) Harnessing a high cargo-capacity transposon for genetic applications in vertebrates. *PLoS Genet.* **2,** e169
51. MacDonald, M. J. (1981) High content of mitochondrial glycerol-3-phosphate dehydrogenase in pancreatic islets and its inhibition by diazoxide. *J. Biol. Chem.* **256,** 8287–8290
52. Takatsu, H., Baba, K., Shima, T., Umino, H., Kato, U., Umeda, M., Nakayama, K., and Shin, H. W. (2011) ATP9B, a P4-ATPase 9a putative aminophospholipid translocase), localizes to the trans-Golgi network in a CDC50 protein-independent manner. *J. Biol. Chem.* **286,** 38159–38167
53. Hasan, N. M., Longacre, M. J., Stoker, S. W., Boonsaen, T., Jitrapakdee, S., Kendrick, M. A., Wallace, J. C., and MacDonald, M. J. (2008) Impaired anaplerosis and insulin secretion in insulinoma cells caused by siRNA-mediated suppression of pyruvate carboxylase. *J. Biol. Chem.* **283,** 28048–28059
54. Dhar, M. S., Yuan, J. S., Elliott, S. B., and Sommardahl, C. (2006) A type IV P-type ATPase affects insulin-mediated glucose uptake in adipose tissue and skeletal muscle in mice. *J. Nutr. Biochem.* **17,** 811–820
55. MacDonald, M. J., Dobrzyn, A., Ntambi, J., and Stoker, S. W. (2008) The role of rapid lipogenesis in insulin secretion: insulin secretagogues acutely alter lipid composition of INS-1 832/13 cells. *Arch. Biochem. Biophys.* **470,** 153–162